

## STRAIN DISTRIBUTION MONITORING OF CFRTP SINGLE-LAP ULTRASONIC WELDING JOINT USING EMBEDDED OPTICAL FIBER SENSOR

D. Wada<sup>1\*</sup>, H. Murayama<sup>1</sup>, K. Kageyama<sup>2</sup>, J. Takahashi<sup>1</sup>, K. Uzawa<sup>1</sup>, H. Igawa<sup>3</sup>

<sup>1</sup> School of Engineering, Systems Innovation, The University of Tokyo, 7-3-1 Hongo, Bunkyo-ku, Tokyo, 113-8656 Japan

<sup>2</sup> School of Engineering, Technology Management for Innovation, The University of Tokyo, 7-3-1 Hongo, Bunkyo-ku, Tokyo, 113-8656 Japan

<sup>3</sup> Japan Aerospace Exploration Agency, 6-13-1 Osawa, Mitaka, Tokyo, 181-0015 Japan

\*daichi\_wd@giso.t.u-tokyo.ac.jp

**Keywords:** carbon fiber reinforced thermoplastic (CFRTP), embedded sensor, fiber Bragg grating, ultrasonic welding joint.

### Abstract

*In this study we used embedded optical fiber distributed sensors for the monitoring of single-lap ultrasonic welding joints, which were manufactured by carbon reinforced thermoplastic (CFRTP) coupons. The reversible property of the thermoplastic resin enables easy embedding of optical fibers into CFRTP coupons and also allows the joining method of ultrasonic welding. A long-length fiber Bragg grating (FBG) was embedded into the surface of a CFRTP coupon in a hot press machine, and we manufactured a CFRTP single-lap ultrasonic welding joint using the CFRTP coupon with the embedded long-length FBG. We monitored strain distributions along the embedded long-length FBG before and after the ultrasonic welding and discussed about a method of joint quality evaluation based on the strain distributions. We also applied tensile loads to the joints. The embedded long-length FBG successfully measured strain distributions of the joint. In this work, optical frequency domain reflectometry (OFDR) was used as the distributed sensing scheme.*

### 1 Introduction

When composite materials are used as components of structures, such as automobiles, assembling of individual composite parts is required. As a result, end structures eventually have many joints. Joint parts tend to become the weakest chain of structures, therefore accurate and effective monitoring of stress/strain fields at joints, especially at joint interfaces, is required for the assurance of structural integrity. Bonding joints are attractive because they achieve light-weight and less stress concentrations. When it comes to the bonding joints, analytical and numerical approaches [1-4], as well as numerical approaches with finite element analysis (FEA) [5-7] have been proposed by many researchers in order to determine the stress/strain distribution inside adhesive layers and at the interface between adherends and adhesive layers. However, it has been difficult to measure stress/strain fields directly from inside the adhesive layers if conventional sensors, such as strain gauges and displacement gauges, are used. Murayama *et al* have demonstrated strain distribution measurements using optical fiber sensors which were embedded at the interface between adherends and adhesive

layers [8]. This study has suggested the applicability of embedded optical fiber sensors for the direct joint monitoring.

Carbon fiber reinforced thermoplastics (CFRTPs) are expected to be the promising material which is recyclable, repairable and capable of high-cycle molding. In the case of CFRTPs, welded joining is available thanks to their reversible material property. Welded joining does not require any alien substances such as adhesives or mechanical fasteners to make a joint, which benefits for example the less weight and cost effectiveness. Ultrasonic welding is one of the welded joining methods, which is capable of short time processing. Ultrasonic welders emit ultrasonic waves, which produce friction heats between surfaces of overlapped CFRTP adherends. Their resins are instantly welded and integrated when they are cooled down. However, results of joints are influenced by welding conditions such as ultrasonic parameters and adherends conditions. Therefore, it is important to establish a monitoring method to evaluate the quality of ultrasonic welding joints before these joints can be used with sufficient reliability.

Optical fiber sensors would be useful for the quality evaluation of manufactured ultrasonic welding joints and the understanding of the mechanical behavior of ultrasonic welding joints in service. If they are embedded into the surface of adherends and ultrasonic welding joints are manufactured, one can implement strain monitoring consistently from the process of joint manufacturing to the mechanical tests at the interface of the joints. Their thin diameter and light-weight enables the minimum intrusion to a structure without disrupting the strain fields around optical fibers. We have developed optical fiber distributed strain measurement system using fiber Bragg gratings (FBGs) based on optical frequency domain reflectometry (OFDR) [9,10]. We employ 10 cm long-length FBGs with low reflectivity. The OFDR system can measure strain or temperature distribution with the high accuracy of  $\pm 5 \mu\epsilon$  or  $\pm 0.5^\circ\text{C}$ , respectively, and with the high spatial resolution of less than 1 mm. This means one can obtain strain or temperature at the arbitrary position with the interval of less than 1 mm along the long-length FBG.

In this study, we prepared CFRTP coupons and embedded the long-length FBG into the surface of the coupon using the hot press machine. We manufactured ultrasonic welding joint using the coupons. We monitored strain distributions along the embedded long-length FBG before and after the ultrasonic welding based on OFDR. We also applied tensile loads to the joint and mechanical behaviors based on measured strain distributions.

## 2 Distributed sensing system based on OFDR using long-length FBGs

We have developed optical fiber distributed sensing system based on OFDR. In this paper, we used long-length FBGs whose length is 10 cm. OFDR enables one to interrogate Bragg spectra at arbitrary locations within the long-length FBGs. We can allocate the long-length FBGs sequentially in optical fibers with minimum gaps, so that we secure sensing region longer than 10 cm.

Figure 1 shows the schematic of the OFDR sensing system. The typical sensing system consists of a tunable laser source, a PC, an A/D converter and two interferometers. The sensing principle of the OFDR system can be explained by an approximated description which is demonstrated by Childers *et al* [11]. This approximated description expresses the obtained signal of detector 2 (D2) as a sum of the reflected spectra from each location along FBGs. This approximation is sufficient for the conceptual introduction and valid because we used low-reflectivity FBGs. The incident light is split at the coupler 1 (C1) and proceeds into Interferometer 1 and 2. In Interferometer 1 propagating lights are reflected by mirrors (M1 and M2). Detector 1(D1) observes the interfered signal of the reflected lights. This signal  $D_1$  is expressed as

$$D_1 = 2 \left\{ 1 + \cos(2n_{eff}L_R k) \right\}, \quad (1)$$

where  $n_{eff}$  is the effective refractive index of the optical fiber,  $L_R$  is the path difference between M1 and M2 and  $k$  is the wavenumber. By triggering  $D_1$ , the constant interval of the wavenumber,  $\Delta k$ , is obtained as

$$\Delta k = \frac{\pi}{n_{eff}L_R}. \quad (2)$$

In Interferometer 2, the signal observed at D2 is sampled by  $\Delta k$ . D2 observes the interfered signal of reflected lights from M3 and the FBG. This signal  $D_2$  is expressed as

$$D_2 = \sum_i R_i(k) \cos(2n_{eff}L_i k), \quad (3)$$

where  $R_i$  is the reflected spectrum in the  $i$ th grating and  $L_i$  is the path difference between  $i$ th grating and M3.  $D_2$  includes the Bragg wavelength information in the term of  $R_i$  and the position information in the frequency. Therefore, one can obtain strain distributions along long-length FBGs by applying signal processing based on short-time Fourier transform (STFT).

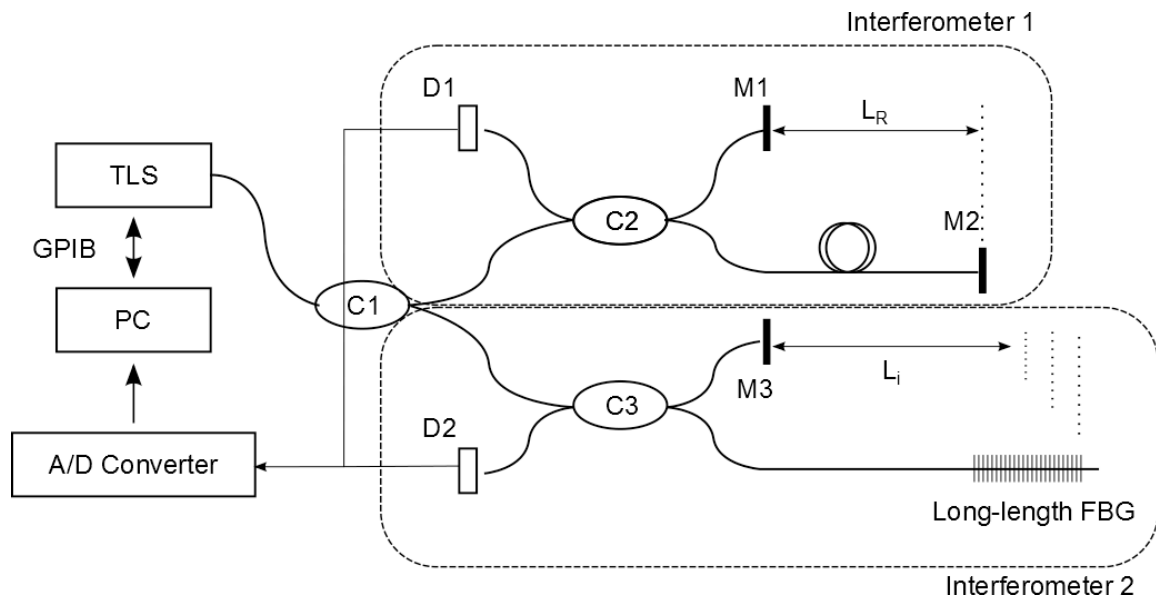


**Figure 1.** Schematic of the OFDR system. TLS: tunable laser source, D: photo diode detector, C: optical 3 dB coupler, M: reflection mirror.

### 3 Ultrasonic welding manufacture and strain distribution monitoring by embedded FBGs

We embedded a long-length FBG into a CFRTP coupon and made an ultrasonic welding joint. We demonstrated strain distribution monitoring using the embedded FBG based on OFDR before and after ultrasonic welding.

Figure 2 shows the schematic of the FBG embedding process. We prepared a CFRTP coupon, which were made of unidirectional CF/PP prepreg. CF was TR50S, provided by Mitsubishi

Rayon. Toyobo provided high-modified PP by maleic acid. We set silicon rubbers at both ends of the coupon in order to stop the resin flow during molding. A Teflon film was inserted between the coupon and an optical fiber in order to keep a certain area of the optical fiber not embedded. We closed the metal molds and applied heat and pressure. The manufactured coupon, which had the optical fiber embedded into the surface, had the length, width and thickness of 200 mm, 24.8 mm and 1.67 mm, respectively.

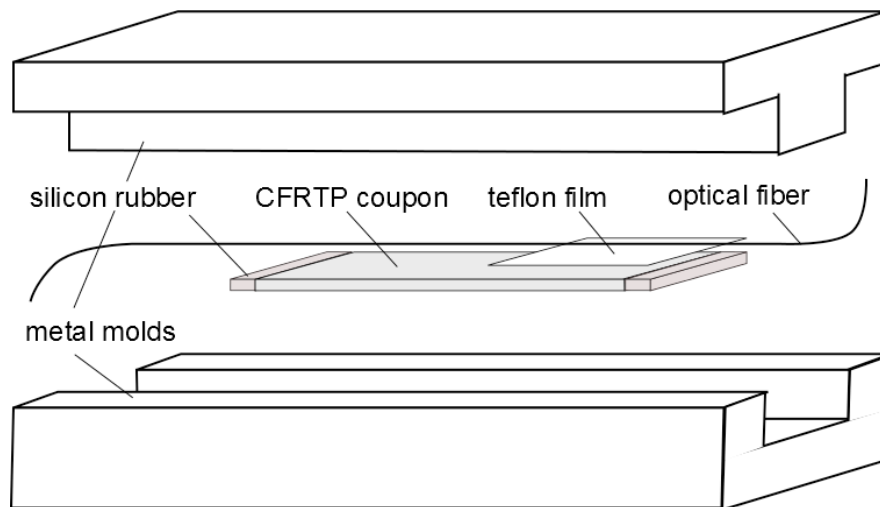


**Figure 2.** Schematic of optical fiber embedment into a CFRTP coupon.

We prepared another CFRTP coupon with the same material whose length, width and thickness were 195 mm, 24.7 mm and 1.66 mm. This coupon did not have embedded optical fibers. We set these two CFRTP coupons, one was with the embedded optical fiber and the other without it, and made ultrasonic welding joint. Figure 3 shows a picture of the ultrasonic welding joint making process. We used the ultrasonic welding machine of Nippon Future Co. Ltd. We applied ultrasonic waves with 20 kHz frequency for 1 second. Pressure and ultrasonic waves are conveyed from the metal horn to two coupons. Friction heat arises at the interface of two coupons, which weld the resin of the coupons and fix them when they are cooled down. Figure 4 expresses the configuration of the manufactured ultrasonic welding joint. The location of the FBG part of the optical fiber is indicated. We used 100 mm long-length FBG. 80 mm of the FBG was embedded into the surface of the coupon, and 30 mm out of the 80 mm was located at the joint interface. 20 mm of the FBG was left not embedded. This “free part” was used for temperature compensation. Tabs were attached at both ends of the joint by the ultrasonic welding.

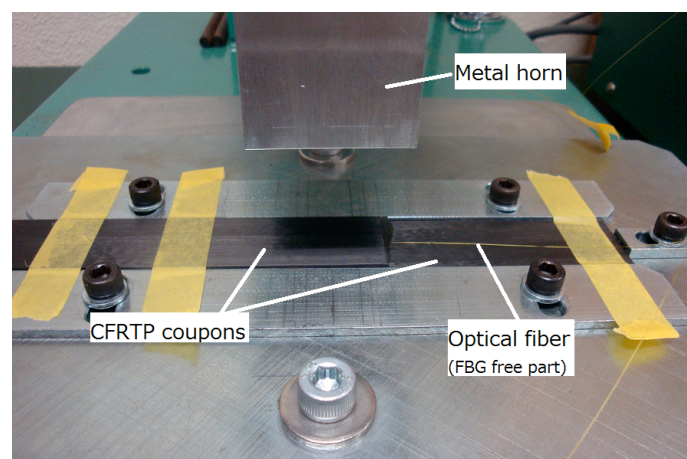


**Figure 3.** Picture of the ultrasonic welding.

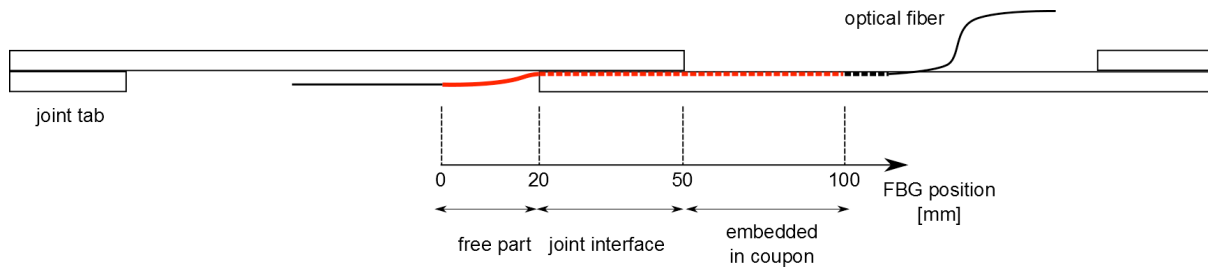


**Figure 4.** Configuration of the manufactured ultrasonic welding joint.

We performed strain distribution measurements using the embedded FBG based on OFDR before and after the ultrasonic welding. The results are shown in fig. 5. Strain distributions were calculated from shifts of Bragg peaks. For the case of the measurement before ultrasonic welding, a tensile strain distribution was observed. This was because the silicon rubbers at two sides fixed the optical fiber, and the fiber was stretched according to the thermal expansion of the metal molds. The tensile strain of the optical fiber remained when the fiber was fixed by the solidification of the CFRTP resin. This means that the tensile strain distribution does not indicate the strain of the coupon itself. The tensile strain gradually decreases towards the end of the coupon. In the case of the measurements after the ultrasonic welding, the strain distribution at the “embedded in coupon surface” area stayed unchanged. On the other hand, the tensile strain was released at the joint interface. Therefore it can be said that the ultrasonic welding method locally welded the joint interface area. The strain release would have occurred when the friction heat welded the resin of the coupon. The tensile strain distribution in the area was relatively uniform, which would suggest there were no obvious fractures occurred during the ultrasonic welding process. Further examination of the relationship between joint quality and strain distributions would be helpful to establish a method of joint quality evaluation by using embedded FBGs.

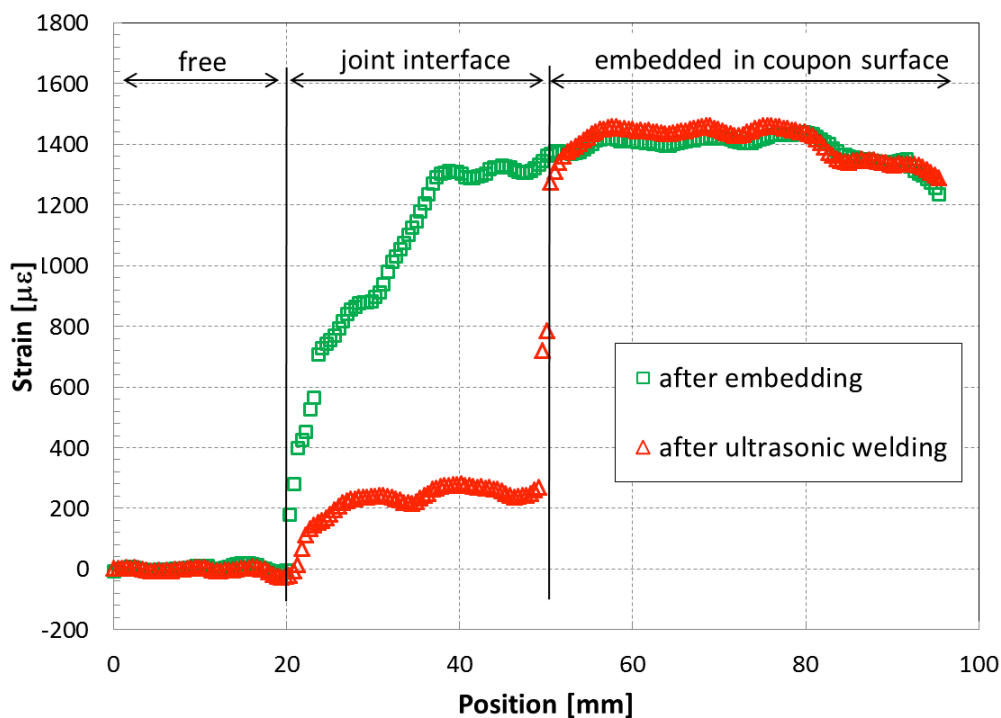


**Figure 5.** Strain distributions before and after ultrasonic welding measured by the embedded long-length FBG.

#### 4 Strain distribution monitoring of the CFRTP single-lap ultrasonic welding joint under tensile loads by the embedded FBG

We applied tensile loads to the CFRTP single-lap ultrasonic welding joint, and measured strain distributions using the embedded FBG based on OFDR. Figure 6 shows the experimental results. Strain distributions indicate the strain variation from the joint condition without loadings. Strain distributions varied at the “joint interface” and the “embedded in coupon surface” areas in accordance with the applied loads. Strain distribution profiles measured by the OFDR system are expected to be in good agreements with calculation results by finite element analysis (FEA). Murayama *et al* have measured strain distributions inside the adhesive layer of the bonded joint using the OFDR system, and their experimental results were in good agreements with FEA results [8]. In this case of the ultrasonic welding joint, however, if a completely integrated joint (seamless joint interface) is assumed and the material nonlinearity is not assumed, the FEA calculation results only match with the experimentally obtained strain distribution profiles at the “embedded in coupon surface” area. At the “joint interface” area, the strain distributions of FEA have steep drop at the edge of the interface (around 40 – 50 mm position in fig.6). Further discussion is required about the finite element model to describe the ultrasonic welding joint accurately. The obtained strain distribution profiles will be helpful to construct the finite element model and understand mechanical properties of the ultrasonic welding joints.

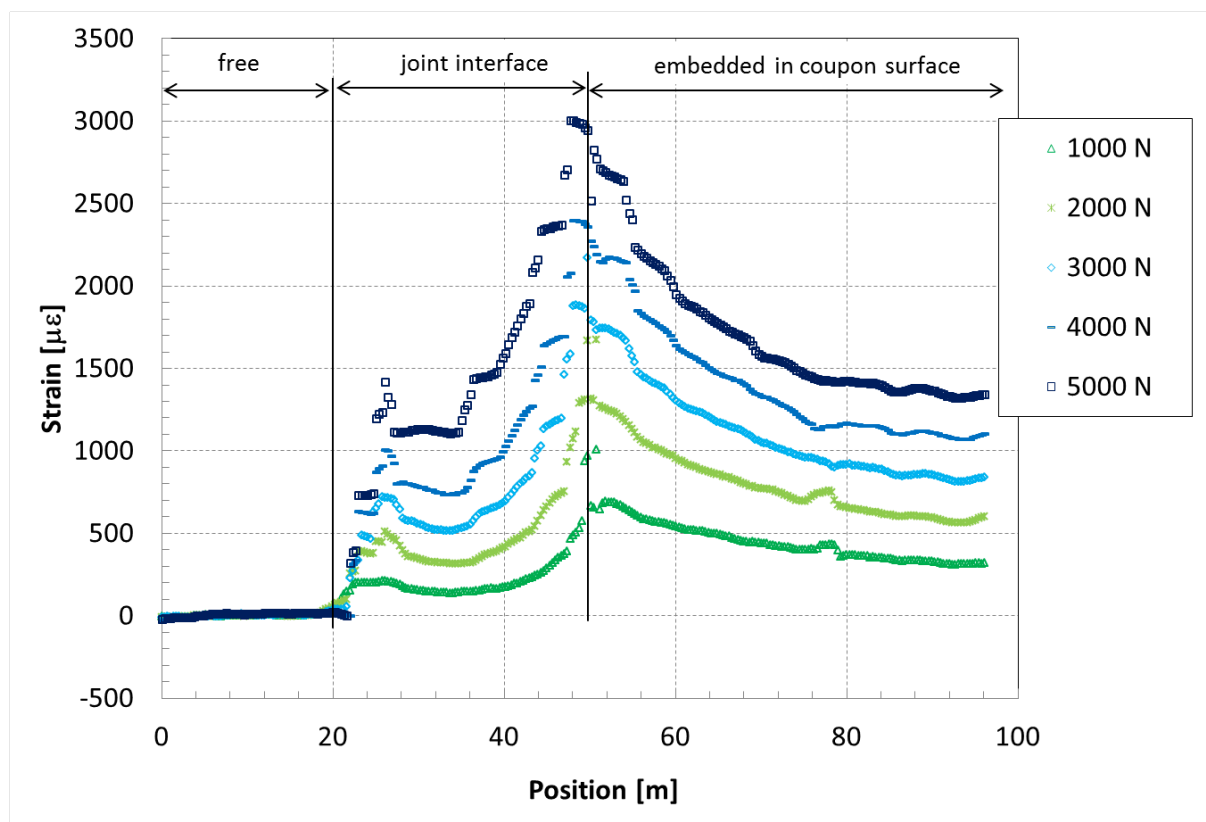


**Figure 6.** Results of strain distribution measurements of the CFRTP single-lap ultrasonic welding joint under tensile loads. Strain variations after the ultrasonic welding joint are calculated.

## 5 Conclusions

We proposed the sensing technique using embedded long-length FBGs and OFDR for the single-lap ultrasonic welding joint monitoring. The joint manufacturing process and the joint under tensile tests were monitored.

We embedded the long-length FBG into the surface of the CFRTP coupon and manufactured the single-lap ultrasonic welding joint. The embedded long-length FBG was interrogated by OFDR sensing system, which enabled us to measure strain distributions along the FBG. The tensile strain remained at the embedded area of the FBG when it was embedded. After ultrasonic welding the tensile strain was released only at the joint interface area. It was indicated that the monitoring of the tensile strain distribution variations before and after the ultrasonic welding could be useful for the joint quality evaluation.

We conducted tensile tests using the CFRTP single-lap ultrasonic welding joint. The strain distributions were measured at each loading case using the embedded FBG. The strain distributions varied in accordance with the applied loads. The strain distribution profiles would be helpful to create the valid finite element model of the joint and understand mechanical properties of the joints.

## Acknowledgement

A part of this work belongs to Japanese METI-NEDO project “Development of sustainable hyper composite technology” since 2008fy.

## References

- [1] Goland M, Reissner E. The stresses in cemented joints. *Journal of Applied Mechanics*, **11**, pp. A17-A27 (1944).
- [2] Hart-Smith L. J. Adhesive bonded single-lap joints –technical report. *NASA-CR-112236* (1973)
- [3] Bigwood W. A., Crocombe A. D. Non-linear adhesive bonded joint design analyses. *International Journal of Adhesion and Adhesives*, **10**, pp. 31-41 (1990)
- [4] Smeltzer III S. S., Klang E. C. *Analysis method for inelastic, adhesively bonded joints with anisotropic adherends* in Proceeding of 18<sup>th</sup> American Society for Composites Technical Conference, Florida, USA (2003)
- [5] Wooley G. R., Carver D. R. Stress concentration factors for bonded lap joint. *Journal of Aircraft*, **8**, pp. 817-820 (1971)
- [6] Tsai M. Y., Morton J. An evaluation of analytical and numerical solutions to the single-lap joint. *International Journal of Solids and Structures*, **31**, pp. 2537-2563 (1994)
- [7] Bogdanovich A. E., Yushmanov S. P. 3-D progressive failure analysis of bonded composite joints. *Collection of Technical Papers – AIAA/ASME/ASCE/AHS/ASC Structures, Structural Dynamics and Materials Conference*, **2**, pp. 1616-1626 (1998)
- [8] Hideaki M., Kazuro K., Kiyoshi U., Kohei O., Hirotaka I. Strain monitoring of a single-lap joint with embedded fiber-optic distributed sensors. *Structural Health Monitoring*, **11**, pp. 325-344 (2011)
- [9] Hirotaka I., Keiichi O., Tokio K., Isao Y., Hideaki M., Kazuro K., Distributed measurements with a long gauge FBG sensor using optical frequency domain reflectometry (1st report, system investigation using optical simulation model). *Journal of Solid Mechanics and Materials Engineering*, **2**, pp.1-11 (2008)
- [10] Hirotaka I., Hideaki M., Toshiya N., Isao Y., Kazuro K., Kiyoshi U., Daichi W., Isam O., Makoto K., Koji O., Measurement of distributed strain and load identification using 1500

mm gauge length FBG and optical frequency domain reflectometry. *Proceedings of SPIE*, **7503**, pp.750351-1-4 (2009)

- [11] Childers B. A., Froggatt M. E., Allison S. G., Moore T. C. Sr., Hare D. A., Batten C. F., Jegley D. C., Use of 3000 Bragg grating strain sensors distributed on four eight-meter optical fibers during static load tests of a composite structure. *Proceedings of SPIE*, **4332**, pp. 133-142 (2001)